

Robustness in Liquid Transfer Vehicles with Delayed Resonators

M. P. TZAMTZI, F. N. KOUMBOULIS, N. D. KOUVAKAS, M. G. SKARPETIS

Department of Automation
Halkis Institute of Technology
34400, Psahna, Evia
GREECE

tzamtzi@teihal.gr, koumboulis@teihal.gr, kouvakas@teihal.gr, skarpetis@teihal.gr

Abstract: - In the present paper, the dynamic model of a liquid transfer vehicle with delayed resonators is modified to take into account simultaneous wear to the front and rear springs. This failure is mathematically formulated as increase to the spring constant with simultaneous decrease to the damping factor. A sloshing suppression control scheme, whose parameters are evaluated using a metaheuristic approach, designed knowing only the nominal values of the resonator parameters while considering their real values to be unknown, is applied to the real system. Then, the sets of resonator parameters where the feedback control law produces satisfactory results are determined, thus verifying robustness of the proposed control scheme.

Key-Words: robustness analysis, liquid transfer, delay resonators, spring wear

1 Introduction

In casting and steel industries, molten metal is usually moved from the furnace to the casting areas using automotive carts that carry tanks filled with the molten metal. A significant problem that has to be solved is the suppression of the liquid's sloshing within the tank. Sloshing is dangerous, since it may cause overflow, as well as deterioration of the product quality due to contamination and excessive cooling of the molten metal [1].

Several studies of sloshing suppression have appeared in the literature (see for example [1]–[12]). Many of these works approximate the liquid's motion using a pendulum-type model ([1]–[5], [8], [10], [11]). Optimal control ([12]), as well as H_∞ control methods ([5], [8]) have been proposed. Active control methods that actuate the rotational motion of the tank have been proposed in [1] and [5]. Both these works considered sloshing suppression during an accelerated translational motion of the vehicle along a straight path, while the proposed controllers used measurements of the liquid level displacement.

Another approach proposed in [13] uses active vibration absorption for sloshing suppression, using delayed resonators (see f.e. [14]–[16]) for the case of liquid transfer using a tank mounted on a vehicle. In particular, a static feedback law is proposed whose parameters are evaluated using a simulated annealing algorithm.

In the present paper, the dynamic model of the plant presented in [13] is modified to take into account simultaneous wear to the front and rear springs of the resonator. This failure is modeled as increase to the spring constant of the resonators with

simultaneous decrease to the damping factor [17]. A sloshing suppression control scheme, whose parameters are evaluated using a metaheuristic approach, designed knowing only the nominal values of the resonator parameters while considering their real values to be unknown, is applied to the real system. Then, robustness of the control scheme is studied under the aforementioned uncertainty in the resonator parameters due to wear. The controller is then applied to the real system whose parameters may vary from the nominal values. The contribution of the present paper consists in determining the sets of resonator parameters where the feedback control law produces satisfactory results.

Another interesting problem concerning robustness issues related to liquid parameter variations in a liquid transfer structure with robotic manipulator has been studied in [18].

The present paper is an extended version of the paper [19].

2 Liquid Transfer Vehicle Modeling

Consider the liquid transfer application presented in Figure 1 (see [13]). The liquid is contained within a tank, carried by an automotive vehicle. Assuming that the vehicle moves on a straight path, the whole motion of the liquid transferring structure can be faced as a two dimensional problem.

The tank may rotate with respect to the vehicle. The rotation of the tank is appropriately controlled through an actuator that applies a torque $u(t)$ to the tank. The vehicle is assumed to move on a horizontal level. Unevenness on the level of the vehicle's

motion is modeled as force disturbances $F_f(t)$ and $F_r(t)$ acting on the front and the rear wheel, respectively, of the vehicle. The vibrations of the vehicle are absorbed by four absorbers, two of which act as active absorbers and the rest act as passive absorbers. The passive absorbers (suspension) are two identical conventional spring-damper structures that connect the platform of the vehicle with the front and the rear wheel, respectively. The active vibration absorbers are two identical mass-spring-

damper trios that utilize position feedback with controlled delay (see f.e. [13]-[15]) and are placed on top of the vehicle's platform at the position of the front and the rear wheel, respectively. The function of the active vibration absorbers is based on a technique called Delayed Resonators [14]-[16]. The equivalent liquid transfer structure, based on the representation of the tank with a rotating joint and the representation of the liquid's motion with a pendulum, is given in Figure 2 (see [13]).

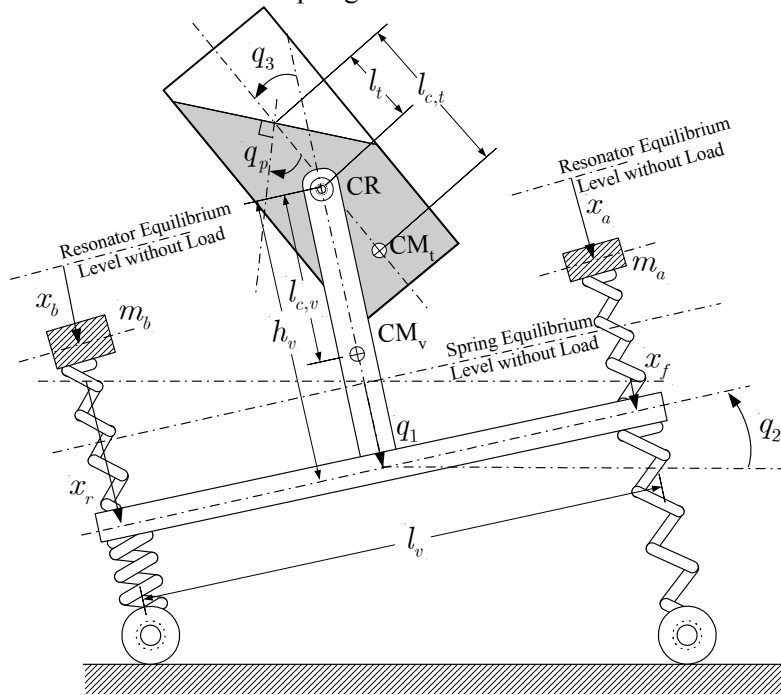


Fig. 1: Liquid transfer application [13]

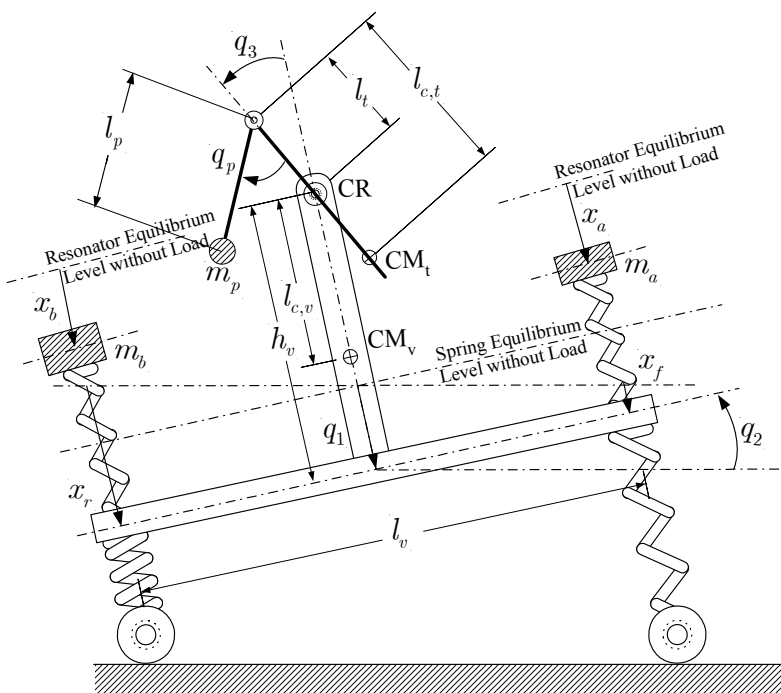


Fig. 2: Representation of liquid's motion with a pendulum [13]

In order to develop the dynamic model of the system, it is assumed that the parameters of the front and rear resonator, as well as the respective control delays are equal. Furthermore, it will be assumed that due to wearing, the spring constants and dumping factors will differ from their nominal values. This difference, although constant and equal to both resonators, will be assumed to be unknown, while only the nominal value of the respective parameter will be known. According to [17], the influence of wear to the springs can be described as increase to the spring constant and decrease to the dumping factor. Let $q = [q_1 \ q_2 \ q_3 \ q_p \ x_a \ x_b]^T$ denote the generalized coordinates of the structure, with q_1 the vertical deviation of the platform from the level corresponding to the natural length of the passive absorbers' spring, q_2 the rotation angle of the vehicle's platform, q_3 the rotation angle of the tank with respect to the vehicle, q_p the rotation of the pendulum with respect to the tank and x_a, x_b the aforementioned deviations of the resonators. Furthermore, let m_p, m_t, m_v and m_{res} be the pendulum, tank, vehicle and resonator masses respectively, h_v and l_v be the vehicle height and length, respectively, $l_{c,v}$ be the distance of the vehicle's center of mass (CM) from the center of revolution (CR), l_t be the distance between CR and the free surface of the liquid, $l_{c,t}$ be the distance of the tank's center of mass (CM) from the free surface of the liquid, l_p be the pendulum length, ψ_r be the free length of the resonator spring, k_{res} be the constant of the resonator spring, k_e be the constant of the suspensions spring, c_{res} be the dumping factor of the resonators, c_e be the dumping factor of the suspensions, c be coefficient of viscosity of the liquid, I_t be the moment of inertia of the tank, I_v be the moment of inertia of the vehicle, g_{res} be the resonator feedback gain, τ be the resonator feedback delay and g be the gravity acceleration. With respect to resonator spring constant and dumping factor it will be assumed that $k_{res} = \bar{k}_{res} + \delta k_{res}$, $c_{res} = \bar{c}_{res} - \delta c_{res}$ where \bar{k}_{res} and \bar{c}_{res} are the known nominal values of the respective parameters and δk_{res} and δc_{res} are unknown constant

perturbations (disturbances) to the respective values due to wear. According to [13], the nonlinear dynamic model of the above presented plant takes on the form:

$$\begin{bmatrix} D(q(t)) & 0_{2 \times 2} \\ 0_{2 \times 2} & I_{2 \times 2} \end{bmatrix} \ddot{q}(t) + \begin{bmatrix} C(q(t), \dot{q}(t)) \\ C_r(q(t), \dot{q}(t)) \end{bmatrix} \dot{q}(t) + \begin{bmatrix} G(q(t), q(t - \tau)) \\ G_r(q(t), q(t - \tau)) \end{bmatrix} = \begin{bmatrix} 0 & 0 & 1 & 0 & 0 & 0 \end{bmatrix}^T u(t) + \begin{bmatrix} \cos(q_2(t)) & \frac{l_v}{2} & 0 & 0 & 0 & 0 \\ \cos(q_2(t)) & \frac{-l_v}{2} & 0 & 0 & 0 & 0 \end{bmatrix}^T \tau_d(t) \quad (2.1)$$

The elements of the matrices $D(q) = [d_{ij}(q)]$, $i, j = 1, \dots, 4$, $C(q(t), \dot{q}(t)) = [c_{ij}(q(t), \dot{q}(t))]$, $i = 1, \dots, 4$, $j = 1, \dots, 6$, $C_r(q(t), \dot{q}(t)) = [c_{r,ij}(q(t), \dot{q}(t))]$, $i = 1, 2$, $j = 1, \dots, 6$, $G(q(t), q(t - \tau)) = [G_i(q(t), q(t - \tau))]$, $i = 1, \dots, 4$ and $G_r(q(t), q(t - \tau)) = [G_{r,i}(q(t), q(t - \tau))]$, $i = 1, 2$ are nonlinear functions of the structure's generalized variables and their respective velocities. Note that $D(q)$ is a symmetric positive definite matrix. The elements of these matrices are given by the following equations [13]:

$$\begin{aligned} d_{11} &= m_v + m_t + m_p \\ d_{12} &= [l_{c,v} m_v - h_v (m_v + m_t + m_p)] \sin(q_2) + [l_{c,t} m_t - l_t (m_t + m_p)] \sin(q_2 + q_3) + l_p m_p \sin(q_2 + q_3 + q_p) \\ d_{13} &= [l_{c,t} m_t - l_t (m_t + m_p)] \sin(q_2 + q_3) + l_p m_p \sin(q_2 + q_3 + q_p) \\ d_{14} &= l_p m_p \sin(q_2 + q_3 + q_p) \\ d_{22} &= I_t + I_v + (l_t^2 + l_p^2 + h_v^2) m_p + \left[(l_{c,t} - l_t)^2 + h_v^2 \right] m_t + (h_v - l_{c,v})^2 m_v + 2h_v [-l_{c,t} m_t + l_t (m_t + m_p)] \cos(q_3) - 2l_p m_p [l_t \cos(q_p) + h_v \cos(q_3 + q_p)] \\ d_{23} &= I_t + (l_t^2 + l_p^2) m_p + (l_{c,t} - l_t)^2 m_t + h_v [-l_{c,t} m_t + l_t (m_t + m_p)] \cos(q_3) - \end{aligned}$$

$$\begin{aligned}
 & l_p m_p [2l_t \cos(q_p) + h_v \cos(q_3 + q_p)] \\
 d_{24} = & l_p m_p [l_p - l_t \cos(q_p) - h_v \cos(q_3 + q_p)] \\
 d_{33} = & I_t + (l_t^2 + l_p^2) m_p + (l_{c,t} - l_t)^2 m_t - \\
 & -2l_p l_t m_p \cos(q_p) \\
 d_{34} = & l_p m_p [l_p - l_t \cos(q_p)], \quad d_{44} = l_p^2 m_p \\
 c_{11} = & (2c_v + 2c_{res}) \cos(q_2(t)) \\
 c_{12} = & \left\{ [l_{c,v} m_v - h_v (m_v + m_t + m_p)] \cos(q_2) + \right. \\
 & [l_{c,t} m_t - l_t (m_t + m_p)] \cos(q_2 + q_3) + \\
 & \left. l_p m_p \cos(q_2 + q_3 + q_p) \right\} \dot{q}_2 + \\
 & \left\{ [l_{c,t} m_t - l_t (m_t + m_p)] \cos(q_2 + q_3) + \right. \\
 & \left. l_p m_p \cos(q_2 + q_3 + q_p) \right\} \dot{q}_3 + \\
 & + l_p m_p \cos(q_2 + q_3 + q_p) \dot{q}_p \\
 c_{13} = & \left\{ [l_{c,t} m_t - l_t (m_t + m_p)] \cos(q_2 + q_3) + \right. \\
 & \left. l_p m_p \cos(q_2 + q_3 + q_p) \right\} (\dot{q}_2 + \dot{q}_3) + \\
 & l_p m_p \cos(q_2 + q_3 + q_p) \dot{q}_p \\
 c_{14} = & l_p m_p \cos(q_2 + q_3 + q_p) (\dot{q}_2 + \dot{q}_3 + \dot{q}_p) \\
 c_{15} = & c_{16} = -c_{res} \cos(q_2(t)), \quad c_{21} = 0 \\
 c_{22} = & \left\{ [l_{c,t} m_t - l_t (m_t + m_p)] \sin(q_3) + \right. \\
 & \left. l_p m_p \sin(q_3 + q_p) \right\} h_v \dot{q}_3 + \\
 & l_p m_p [l_t \sin(q_p) + h_v \sin(q_3 + q_p)] \dot{q}_p + \\
 & \frac{1}{2} (c_v + c_{res}) l_v^2 / \cos^2(q_2) \\
 c_{23} = & \left\{ [l_{c,t} m_t - l_t (m_t + m_p)] \sin(q_3) + \right. \\
 & \left. l_p m_p \sin(q_3 + q_p) \right\} h_v (\dot{q}_2 + \dot{q}_3) + \\
 & l_p m_p [l_t \sin(q_p) + h_v \sin(q_3 + q_p)] \dot{q}_p \\
 c_{24} = & l_p m_p [l_t \sin(q_p) + h_v \sin(q_3 + q_p)] \times \\
 & (\dot{q}_2 + \dot{q}_3 + \dot{q}_p) \\
 c_{25} = & -c_{26} = -\frac{1}{2} l_v c_{res}, \quad c_{31} = 0 \\
 c_{32} = & \left\{ [-l_{c,t} m_t + l_t (m_t + m_p)] \sin(q_3) - \right. \\
 & \left. l_p m_p \sin(q_3 + q_p) \right\} h_v \dot{q}_2 + l_p l_t m_p \sin(q_p) \dot{q}_p \\
 c_{33} = & l_p l_t m_p \sin(q_p) \dot{q}_p \\
 c_{34} = & l_p l_t m_p \sin(q_p) (\dot{q}_2 + \dot{q}_3 + \dot{q}_p)
 \end{aligned}$$

$$\begin{aligned}
 c_{35} = & c_{36} = c_{41} = 0 \\
 c_{42} = & -l_p m_p [l_t \sin(q_p) + h_v \sin(q_3 + q_p)] \dot{q}_2 + \\
 & + l_t \sin(q_p) \dot{q}_3 \\
 c_{43} = & -l_p l_t m_p \sin(q_p) (\dot{q}_2 + \dot{q}_3) \\
 c_{44} = & c l_p^2 \cos^2(q_2(t) + q_3(t) + q_p(t)) \\
 c_{45} = & c_{46} = 0 \\
 c_{r,11} = & -c_{r,15} = c_{r,21} = -c_{r,26} = -\frac{c_{res}}{m_{res}} \\
 c_{r,12} = & -c_{r,22} = -\frac{c_{res} l_v}{2m_{res} \cos^2(q_2)} \\
 c_{r,13} = & c_{r,14} = c_{r,16} = c_{r,23} = c_{r,24} = c_{r,25} = 0 \\
 g_1(q(t), q(t-\tau)) = & g(m_v + m_t + m_p) + \\
 & 2(k_e + k_{res}) q_1(t) \cos(q_2(t)) - \\
 & k_{res} [x_a(t) + x_b(t)] \cos(q_2(t)) \\
 & - g_{res} [x_a(t-\tau) + x_b(t-\tau)] \\
 g_2(q(t), q(t-\tau)) = & g [l_{c,v} m_v - h_v (m_v + m_t + m_p)] \\
 & \sin(q_2(t)) + g [l_{c,t} m_t - l_t (m_t + m_p)] \times \\
 & \sin(q_2(t) + q_3(t)) + g l_p m_p \sin(q_2(t) + q_3(t) + q_p(t)) \\
 & \frac{1}{2} (k_e + k_{res}) l_v^2 \tan(q_2(t)) - \frac{1}{2} k_{res} l_v [x_a(t) - x_b(t)] \\
 & g m_{res} [2\psi_r + x_a(t) + x_b(t)] \sin(q_2(t)) - \\
 & \frac{1}{2} g_{res} l_v [x_a(t-\tau) - x_b(t-\tau)] \\
 g_3(q(t), q(t-\tau)) = & g [l_{c,t} m_t - l_t (m_t + m_p)] \sin(q_2(t) \\
 & + q_3(t)) + g l_p m_p \sin(q_2(t) + q_3(t) + q_p(t)) \\
 g_4(q(t), q(t-\tau)) = & g l_p m_p \sin(q_2(t) + q_3(t) + q_p(t)) \\
 g_{r,1}(q(t), q(t-\tau)) = & \frac{g_{res}}{m_{res}} x_a(t-\tau) + g \cos(q_2(t)) + \\
 & \frac{k_{res}}{m_{res}} [-q_1(t) - \frac{1}{2} l_v \tan(q_2(t)) + x_a(t)] \\
 g_{r,2}(q(t), q(t-\tau)) = & \frac{g_{res}}{m_{res}} x_b(t-\tau) + g \cos(q_2(t)) + \\
 & \frac{k_{res}}{m_{res}} [-q_1(t) + \frac{1}{2} l_v \tan(q_2(t)) + x_b(t)]
 \end{aligned}$$

The control input of the structure is the torque $u(t)$ that actuates the joint representing the tank's motion, while the disturbance vector

$$\tau_d(t) = [\tau_{d,1}(t) \quad \tau_{d,2}(t)]^T$$

is given by $\tau_{d,1}(t) = F_f(t)$, $\tau_{d,2}(t) = F_r(t)$, where as already mentioned F_f and F_r are disturbance forces that act on the front and the rare wheel, respectively, along the direction of the passive absorbers' springs.

3 Controller Design

Consider the linear static output measurement feedback controller

$$r(t) = [f_1 \quad f_2 \quad f_3] [q_2(t) \quad q_3(t) \quad \dot{q}_3(t)]^T \quad (3.1)$$

where $f_i, i = 1, 2, 3$ the controller parameters to be determined. As was shown in [13], the simplicity of the controller makes it suitable for the application of the simulated annealing technique. The simulated annealing algorithm will be used assuming that $\delta k_{res} = 0$ and $\delta c_{res} = 0$. In what follows the algorithm presented in [20] will be used, appropriately modified, to solve the problem at hand. For other applications of this metaheuristic algorithm, see for example [21] and [22]. For other heuristic optimization approaches, see for example [23] and the references therein.

For the present case, the metaheuristic algorithm of [20] will be applied upon the linearized model of the plant, which takes on the form [13]

$$\dot{x}(t) = Ax(t) + A_d x(t - \tau) + Br(t) + J\xi(t) \quad (3.2)$$

where

$$\begin{aligned} x &= [x_1 \quad x_2 \quad x_3 \quad x_4 \quad x_5 \quad x_6 \quad \vdots \\ &\quad \vdots \quad x_7 \quad x_8 \quad x_9 \quad x_{10} \quad x_{11} \quad x_{12}]^T = \\ &= [\delta q_1 \quad \delta q_2 \quad \delta q_3 \quad \delta q_p \quad \delta x_a \quad \delta x_b \quad \vdots \\ &\quad \vdots \quad \delta \dot{q}_1 \quad \delta \dot{q}_2 \quad \delta \dot{q}_3 \quad \delta \dot{q}_p \quad \delta \dot{x}_a \quad \delta \dot{x}_b]^T \\ r &= \delta u, \quad \xi = [\xi_1, \xi_2]^T = [\delta F_f, \delta F_r]^T \\ A &= \begin{bmatrix} 0_{6 \times 6} & I_6 \\ \tilde{A}_{2,1} & \tilde{A}_{2,2} \end{bmatrix} \end{aligned}$$

$$\tilde{A}_{2,1} = \begin{bmatrix} a_{7,1} & 0 & 0 & 0 & a_{7,5} & a_{7,6} \\ 0 & a_{8,2} & a_{8,3} & a_{8,4} & a_{8,5} & a_{8,6} \\ 0 & a_{9,2} & a_{9,3} & a_{9,4} & a_{9,5} & a_{9,6} \\ 0 & a_{10,2} & a_{10,3} & a_{10,4} & a_{10,5} & a_{10,6} \\ a_{11,1} & a_{11,2} & 0 & 0 & a_{11,5} & 0 \\ a_{12,1} & a_{12,2} & 0 & 0 & 0 & a_{12,6} \end{bmatrix}$$

$$\tilde{A}_{2,2} = \begin{bmatrix} a_{7,7} & 0 & 0 & 0 & a_{7,11} & a_{7,12} \\ 0 & a_{8,8} & 0 & a_{8,10} & a_{8,11} & a_{8,12} \\ 0 & a_{9,8} & 0 & a_{9,10} & a_{9,11} & a_{9,12} \\ 0 & a_{10,8} & 0 & a_{10,10} & a_{10,11} & a_{10,12} \\ a_{11,7} & a_{11,8} & 0 & 0 & a_{11,11} & 0 \\ a_{12,7} & a_{12,8} & 0 & 0 & 0 & a_{12,12} \end{bmatrix}$$

$$\tilde{A}_d = \begin{bmatrix} 0_{6 \times 1} & 0_{6 \times 1} \\ (a_d)_{7,1} & (a_d)_{7,2} \\ (a_d)_{8,1} & (a_d)_{8,2} \\ (a_d)_{9,1} & (a_d)_{9,2} \\ (a_d)_{10,1} & (a_d)_{10,2} \\ (a_d)_{11,1} & 0 \\ 0 & (a_d)_{12,2} \end{bmatrix},$$

$$A_d = [0_{12 \times 4} \quad \tilde{A}_d \quad 0_{12 \times 6}] B = \begin{bmatrix} 0_{7 \times 1} \\ b_{8,1} \\ b_{9,1} \\ b_{10,1} \\ 0 \\ 0 \end{bmatrix}, \quad J = \begin{bmatrix} 0_{6 \times 1} & 0_{6 \times 1} \\ \dot{j}_{7,1} & \dot{j}_{7,2} \\ \dot{j}_{8,1} & \dot{j}_{8,2} \\ \dot{j}_{9,1} & \dot{j}_{9,2} \\ \dot{j}_{10,1} & \dot{j}_{10,2} \\ 0 & 0 \\ 0 & 0 \end{bmatrix}$$

Note that $\delta y = y - y_0$ denotes the deviation of the variable y from the corresponding equilibrium value y_0 . It can readily be observed that

$$\begin{aligned} q_{2,0} &= q_{3,0} = q_{p,0} = \dot{q}_{1,0} = \dot{q}_{2,0} = \\ &= \dot{q}_{3,0} = \dot{q}_{p,0} = \dot{x}_{a,0} = \dot{x}_{b,0} = 0 \\ u_0 &= \xi_{1,0} = \xi_{2,0} = 0 \\ q_{1,0} &= - \frac{g(m_v + m_t + m_p + 2m_{res})}{2k_e} \\ x_{a,0} &= x_{b,0} = \\ &= - \frac{g[2k_e m_{res} + \bar{k}_{res} (m_v + m_t + m_p + 2m_{res})]}{2k_e (g_{res} + \bar{k}_{res})} \end{aligned}$$

The simulated annealing algorithm takes on the form (see also [13]):

Initial data of the algorithm

- Center values and half widths for the initial search area of the controller parameters $f_{1,c}$, $f_{2,c}$, $f_{3,c}$, $f_{1,w}$, $f_{2,w}$ and $f_{3,w}$.
- Desired properties of the closed-loop system
- Actuator, state and/or output variable constraints
- Sampling period T
- Time window range N
- Performance criterion $J(x, u, \xi)$
- Loop repetition parameters n_{loop} , n_{rep} and n_{tot}
- Search algorithm thresholds λ_{f_1} , λ_{f_2} and λ_{f_3}
- External command used for simulation

Search algorithm

Step 1. Set the numbering index $i_{max} = 0$. Set $J_{total\ min} = \infty$.

Step 2. Set the numbering index $i_1 = 0$.

Step 3. Determine a search area \mathfrak{S} for the controller parameters. The search area is bounded according to the inequalities

$$f_{1,\min} \leq f_1 \leq f_{1,\max}, f_{2,\min} \leq f_2 \leq f_{2,\max}$$

$$f_{3,\min} \leq f_3 \leq f_{3,\max}$$

where

$$f_{1,\min} = f_{1,c} - f_{1,w}, f_{2,\min} = f_{2,c} - f_{2,w}$$

$$f_{3,\min} = f_{3,c} - f_{3,w}, f_{1,\max} = f_{1,c} + f_{1,w}$$

$$f_{2,\max} = f_{2,c} + f_{2,w}, f_{3,\max} = f_{3,c} + f_{3,w}$$

Step 4. Set $i_{max} = i_{max} + 1$. If $i_{max} > n_{total}$ go to Step 17.

Step 5. Set the numbering index $i_2 = 0$.

Step 6. Select randomly a set of controller parameters within the search area \mathfrak{S} .

Step 7. Check if the closed-loop system satisfies the desired closed-loop properties. If no, set $J = \infty$ and go to Step 10.

Step 8. Perform simulation of the closed-loop system resulting by applying controller (3.1) to the system (3.2). Use the simulation results for a sufficiently large time window $0 \leq t \leq NT$ and with an appropriate sampling period T , to check if the control input variables $u(kT)$, the state variables $x(kT)$ and the output variable $y(kT)$, $k = 0, \dots, N$ satisfy the actuator, state and/or output constraints. If no, set $J = \infty$ and go to Step 10.

Step 9. Use the simulation results of Step 8 to compute the value of $J(x, u, \xi)$

Step 10. Set $i_2 = i_2 + 1$. If $i_2 \leq n_{loop}$ go to Step 6.

Step 11. Use the results of the last n_{loop} repetitions of Steps 6 - 9 to determine the suboptimal controller that resulted in the smallest value J_{i+1} of the cost criterion.

Step 12. Set $i_1 = i_1 + 1$. If $i_1 \leq n_{rep}$ go to Step 5.

Step 13. Find

$$J_{\min} = \min \{J_i, i = 1, \dots, n_{rep}\}$$

$$J_{\max} = \max \{J_i, i = 1, \dots, n_{rep}\}$$

and the corresponding controller parameters $(f_1)_{J_{\min}}$, $(f_2)_{J_{\min}}$, $(f_3)_{J_{\min}}$, $(f_1)_{J_{\max}}$, $(f_2)_{J_{\max}}$ and $(f_3)_{J_{\max}}$.

Step 14. If $J_{\min} = \infty$ then set

$$f_{1,w} = 2f_{1,w}, f_{2,w} = 2f_{2,w}, f_{3,w} = 2f_{3,w}$$

and go to Step 2. If $J_{\min} < J_{total\ min}$, set $J_{total\ min} = J_{\min}$ and

$$f_{1,total\ min} = (f_1)_{J_{\min}}, f_{2,total\ min} = (f_2)_{J_{\min}}$$

$$f_{3,total\ min} = (f_3)_{J_{\min}}$$

Otherwise, set $J_{\min} = J_{total\ min}$ and

$$(f_1)_{J_{\min}} = f_{1,total\ min}, (f_2)_{J_{\min}} = f_{2,total\ min}$$

$$(f_3)_{J_{\min}} = f_{3,total\ min}$$

Step 15. Define

$$d_{f_1} = \left| (f_1)_{J_{\min}} - (f_1)_{J_{\max}} \right|, d_{f_2} = \left| (f_2)_{J_{\min}} - (f_2)_{J_{\max}} \right|$$

$$d_{f_3} = \left| (f_3)_{J_{\min}} - (f_3)_{J_{\max}} \right|$$

Let

$$f_{1,\min} = (f_1)_{J_{\min}} - d_{f_1}, f_{2,\min} = (f_2)_{J_{\min}} - d_{f_2}$$

$$f_{3,\min} = (f_3)_{J_{\min}} - d_{f_3}, f_{1,\max} = (f_1)_{J_{\min}} + d_{f_1}$$

$$f_{2,\max} = (f_2)_{J_{\min}} + d_{f_2}, f_{3,\max} = (f_3)_{J_{\min}} + d_{f_3}$$

If $|f_{1,\max} - f_{1,\min}| > \lambda_{f_1}$ or $|f_{2,\max} - f_{2,\min}| > \lambda_{f_2}$ or $|f_{3,\max} - f_{3,\min}| > \lambda_{f_3}$, go to Step 2

Step 16. End of the algorithm. If $J_{total\ min} < \infty$, use the controller parameter values $f_{1,total\ min}$, $f_{2,total\ min}$ and $f_{3,total\ min}$. Otherwise the algorithm has failed.

It is important to note at this point that the stability of the linearized closed-loop system is tested at Step 7, since stability is an indispensable desired closed-loop property, which should be definitely included within the desired closed-loop properties specified at the algorithm's initialization phase. Moreover, as it is well known, closed-loop stability of the linearized

system guarantees local closed-loop stability for the corresponding non-linear system, which implies that stability is guaranteed in the vicinity of the corresponding equilibrium point.

In order to demonstrate the efficiency of the controller as well as the metaheuristic algorithm, assume that (see also [13])

$$\begin{aligned}
 m_p &= 2.744 \text{ [kgr]}, m_t = 1.68 \text{ [kgr]} \\
 m_v &= 15.20 \text{ [kgr]}, m_{res} = 0.77 \text{ [kgr]} \\
 h_v &= 0.30 \text{ [m]}, l_v = 0.50 \text{ [m]}, l_{c,v} = 0.304 \text{ [m]} \\
 l_t &= 0.033 \text{ [m]}, l_{c,t} = 0.113 \text{ [m]} \\
 l_p &= 0.0442 \text{ [m]}, \psi_r = 0.10 \text{ [m]} \\
 \bar{k}_{res} &= 52000 \text{ [N/m]}, k_e = 62000 \text{ [N/m]} \\
 \bar{c}_{res} &= 16 \text{ [kgr/sec]}, c_e = 2500 \text{ [kgr/sec]} \\
 c &= 1.88 \text{ [N sec/m]}, I_t = 7.193 \cdot 10^{-3} \text{ [kgr m}^2\text{]} \\
 I_v &= 0.329967 \text{ [kgr m}^2\text{]}, g_{res} = 32976 \text{ [N/m]} \\
 \tau &= 0.0195 \text{ [sec]}, g = 9.81 \text{ [m/sec}^2\text{]} \\
 F_f(t) &= \begin{cases} 1000 \text{ [N]} & 0 \leq t \leq 0.5 \text{ [sec]} \\ 0 \text{ [N]} & t > 0.5 \text{ [sec]} \end{cases} \\
 F_r(t) &= F_f(t - 0.25)
 \end{aligned}$$

while for the metaheuristic algorithm assume that

$$\begin{aligned}
 f_{1,\min} &= -60, f_{1,\max} = 0, f_{2,\min} = -10 \\
 f_{2,\max} &= 0, f_{3,\min} = -2.5, f_{3,\max} = 0 \\
 n_{loop} &= 100, n_{rep} = 10, N = 15000 \\
 T &= 0.001 \text{ [sec]}, \lambda = 0.00001
 \end{aligned}$$

For the closed loop performance to be considered satisfactory, a condition is necessary to be met concerning the maximum allowable angle of the pendulum. More specifically, the maximum absolute value of the pendulum's angle has to remain smaller than or equal to 51.696° . This angle limitation does not allow the free surface of the fluid to approach closer than 1 [cm] to the edges of the tank. The performance criterion will be considered to be of the form

$$J(x, u, \xi) = \|x_2(k)\|_2 \quad (3.3)$$

For these parameter values, the controller parameters that achieve satisfactory sloshing suppression have been determined in [13] to be:

$$\begin{aligned}
 f_1 &= -73.1285, f_2 = -11.27006 \\
 f_3 &= -0.01937
 \end{aligned}$$

It must be noted that parameters of controller (3.1) were determined considering that $k_{res} = \bar{k}_{res}$ and $c_{res} = \bar{c}_{res}$. With respect to efficiency of the search algorithm, it has been observed that it had converged to the controller parameters after 9000 repetitions. Nevertheless, it must be noted that the search algorithm thresholds are quite strict and the controller has practically converged much sooner while the closed loop performance response remains practically unchanged. Indicatively, in Table 1 the center values and half widths of the controller parameters are presented. Indeed, it can be observed that the response characteristics remain practically unchanged after the fourth loop. Note that the all response parameters are evaluated using the sampled data.

Repetition	$f_{1,c}$	$f_{2,c}$	$f_{4,c}$	$f_{1,w}$	$f_{2,w}$	$f_{3,w}$	Cost
1	-57.1415	-9.08794	-0.02713	32.80708	1.897013	0.125018	98.26337
2	-58.9868	-9.72769	-0.03088	9.718936	1.147686	0.048136	89.69127
3	-67.6406	-10.7424	-0.01881	5.473802	0.637211	0.022937	86.66839
4	-72.8916	-11.2102	-0.02078	0.677065	0.038506	0.00561	85.62089
5	-73.0781	-11.2468	-0.01894	0.036232	0.020287	0.000604	85.57291
6	-73.108	-11.2659	-0.01947	0.020413	0.00282	3.08E-05	85.55719
7	-73.1283	-11.2687	-0.01944	0.000218	0.0013	4.64E-05	85.55463
8	-73.1285	-11.27	-0.01941	2.26E-05	0.000114	3.33E-05	85.55422
9	-73.1286	-11.2701	-0.01938	1.98E-06	1.33E-05	9.22E-06	85.55416

Table 1: Metaheuristic Algorithm Parameters and Closed Loop Cost Criterion

To demonstrate the performance of the proposed control scheme, consider the nonlinear model (2.1)

and the data presented previously, assuming that $\delta k_{res} = 0$ and $\delta c_{res} = 0$. In Figures 3 to 14 the

response of the closed loop system is presented, compared to the response of the open loop one. In particular it can readily be observed from Figure 3 that the maximum angular displacement q_p of the pendulum for the closed loop case is significantly smaller than the corresponding open loop value. Furthermore, the oscillations are damped significantly faster, thus achieving satisfactory sloshing suppression. Similarly, in Figure 4, the angular displacement q_3 of the revolutionary joint is presented, which also settles sufficiently fast. With respect to the displacements q_1 and q_2 (see Figures 5 and 6) it can be observed that they are damped fast both in the closed and open loop case. With respect to the displacements of the resonators, it can be observed that they remain within acceptable levels (see Figures 7 and 8). The above conclusions can be made also for the velocities of the respective variables (see Figures 9 to 14). Finally, in Figure 15, the actuatable input u is presented. It must be noted that the required torque is within acceptable limits, thus being easily implementable. It must be noted that some figures have been zoomed to particular areas in order to demonstrate specific details.

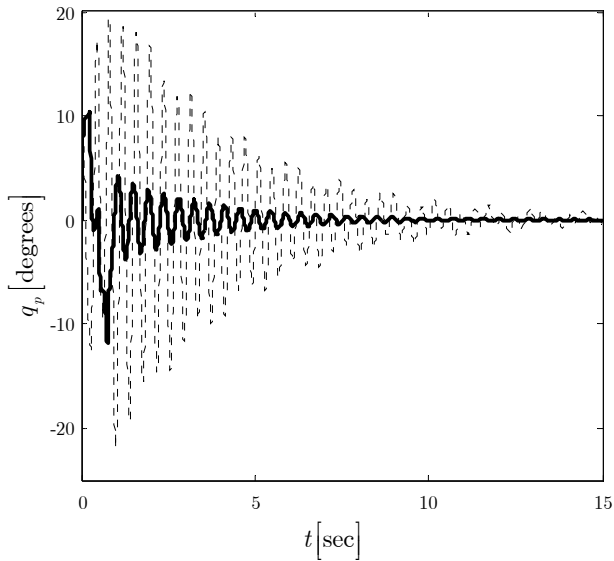


Fig. 3: Pendulum angle q_p
(dotted – open loop, continuous –closed loop)

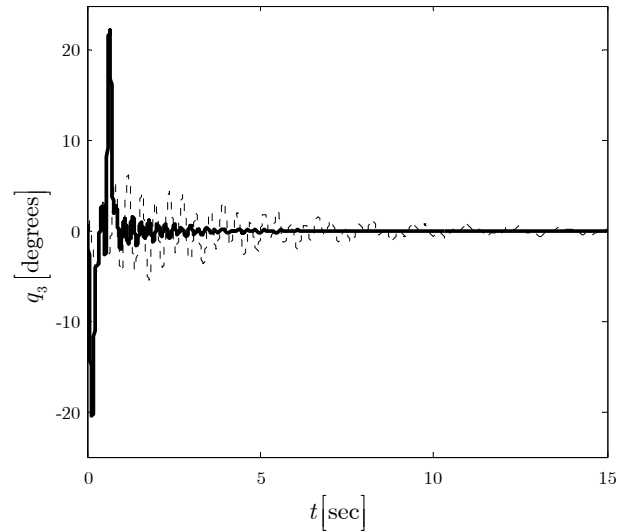


Fig. 4: Angular displacement q_3 of the tank
(dotted – open loop, continuous –closed loop)

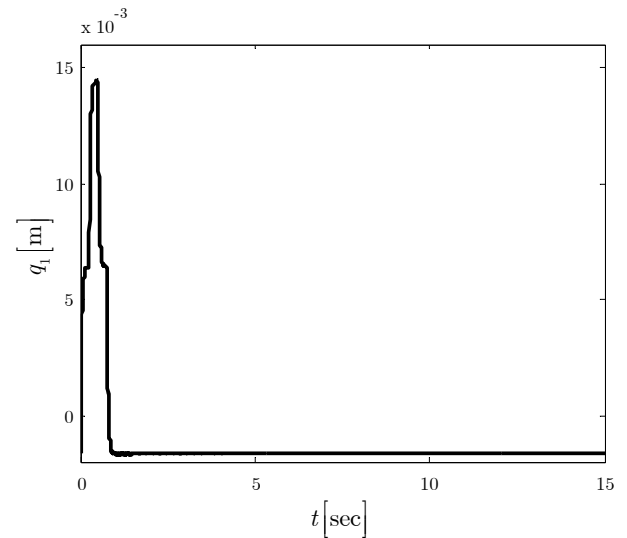


Fig. 5: Open and closed loop vertical deviation q_1 of the platform
(visually identical)

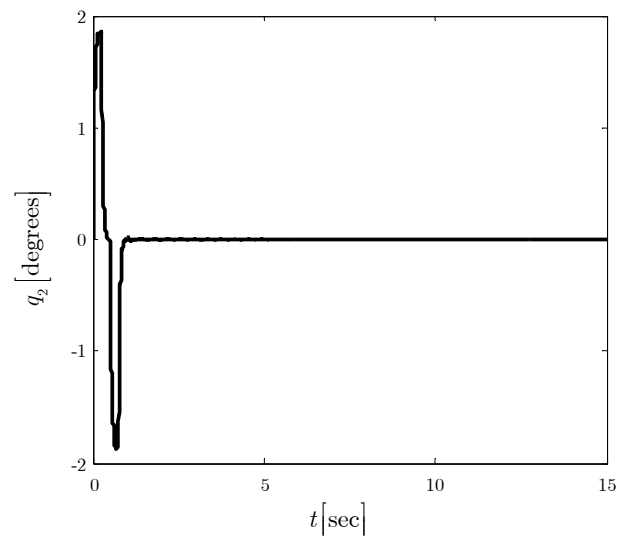


Fig. 6: Open and closed loop rotation angle q_2 of the vehicle's platform
(visually identical)

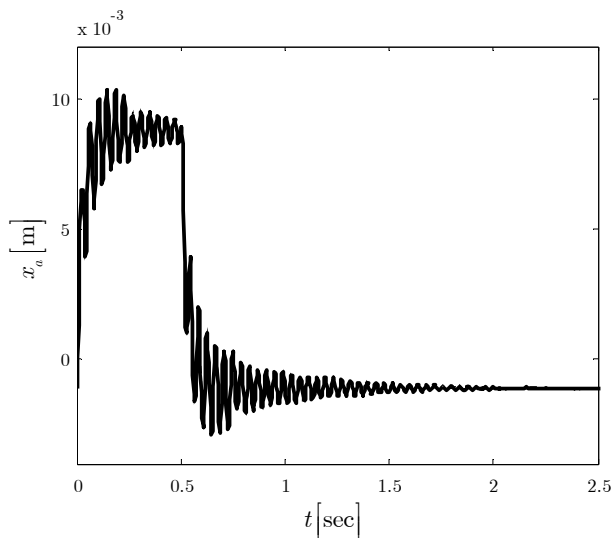


Fig. 7: Open and closed loop front resonator deviation x_a
(visually identical)

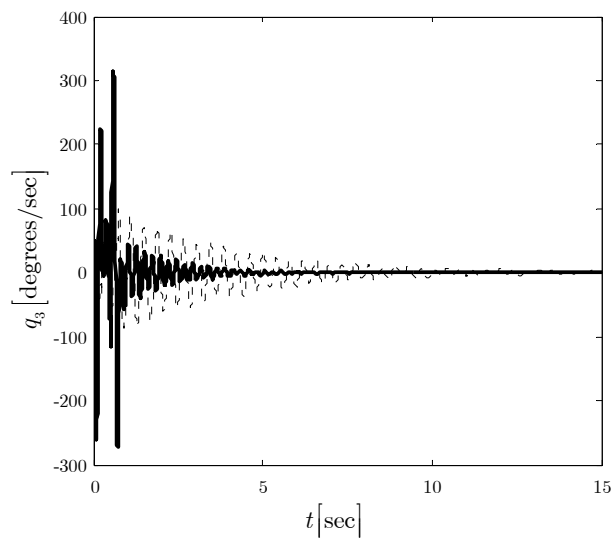


Fig. 10: Angular displacement velocity \dot{q}_3 of the tank
(dotted – open loop, continuous –closed loop)

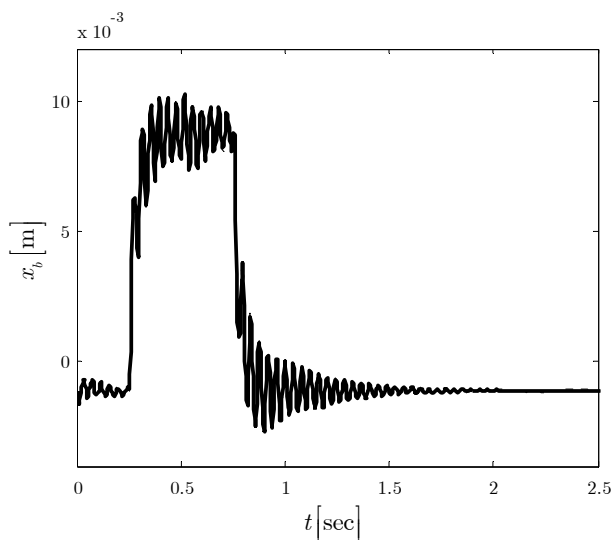


Fig. 8: Open and closed loop rear resonator deviation x_b
(visually identical)

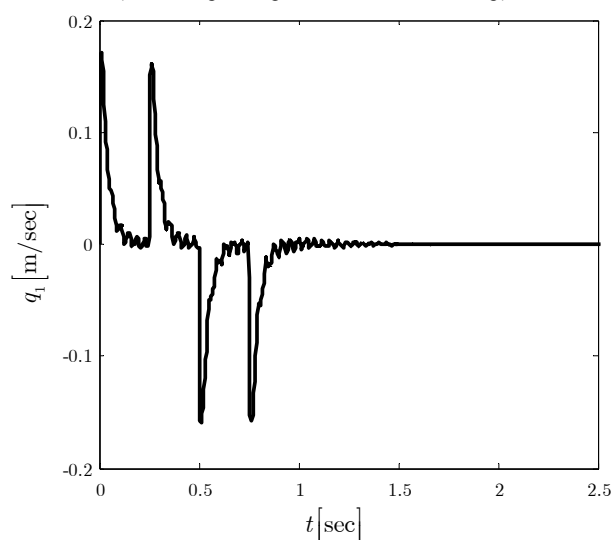


Fig. 11: Open and closed loop vertical deviation velocity \dot{q}_1 of the platform
(visually identical)

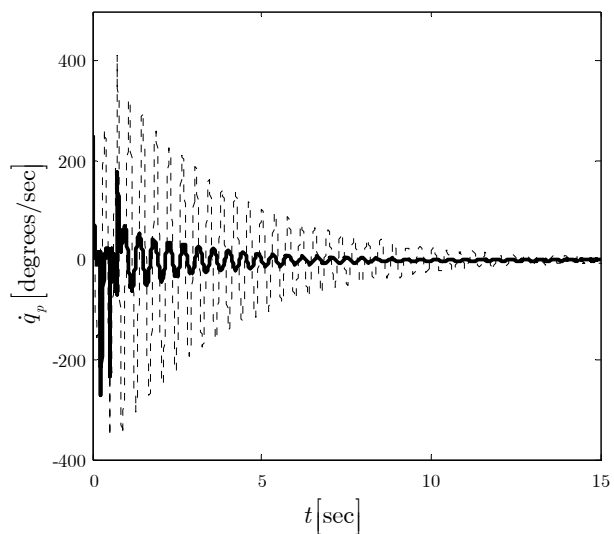


Fig. 9: Pendulum angle velocity \dot{q}_p
(dotted – open loop, continuous –closed loop)

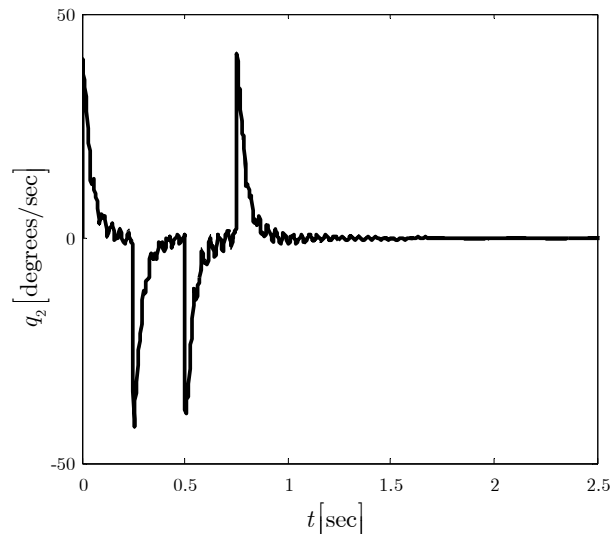


Fig. 12: Open and closed loop rotation angle velocity \dot{q}_2 of the vehicle's platform
(visually identical)

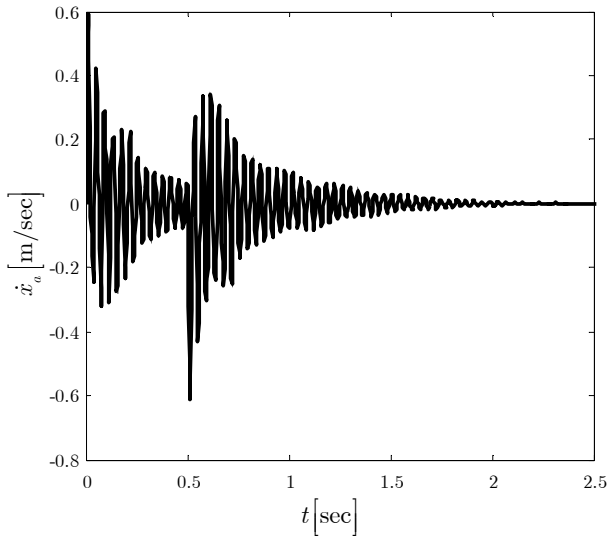


Fig. 13: Open and closed loop front resonator deviation velocity \dot{x}_a (visually identical)

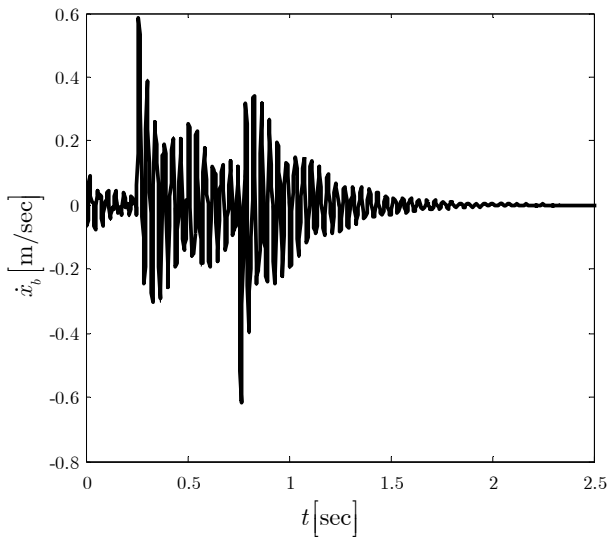


Fig. 14: Open and closed loop rear resonator deviation velocity \dot{x}_b (visually identical)

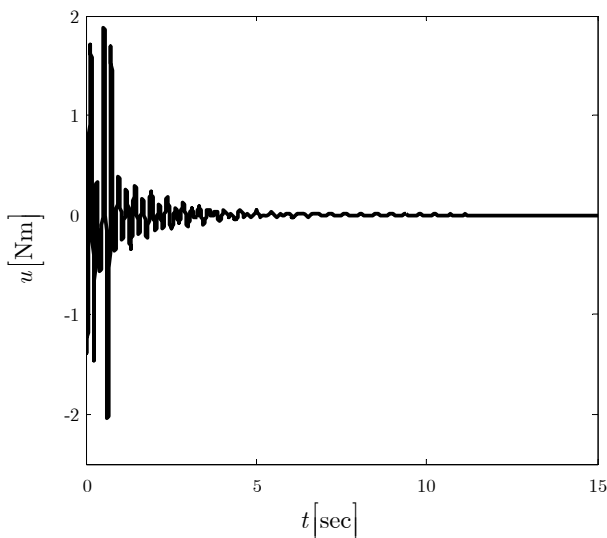


Fig. 15: Actuable input u

4 Robustness Analysis of the Closed Loop System

The robustness of the closed loop system will be examined for the following range of uncertainty:

$$\delta c_{res} \in [13.6, \bar{c}_{res}] \quad \text{and} \quad \delta k_{res} \in [\bar{k}_{res}, 59800].$$

Assuming that this limitation holds, the robustness of the closed loop system in each case will be examined using the following cost criteria

$$f_1(\delta k_{res}, \delta c_{res}) = \sqrt{\int_0^\infty q_p(t)^2 dt} \quad (4.1a)$$

$$f_2(\delta k_{res}, \delta c_{res}) = \sqrt{\int_0^\infty q_3(t)^2 dt} \quad (4.1b)$$

The integrals in criteria (4.1) are guaranteed to converge to some value. This is because the steady state values of $q_p(t)$ and $q_3(t)$ are equal to zero.

Using simulation results for several values of the uncertain parameters, we determine an area of the $(\delta k_{res}, \delta c_{res})$ plane where the maximum pendulum angle condition is met. This area is presented in Figure 16. From Figure 16 it can be observed that this area covers a significant range in the $(\delta k_{res}, \delta c_{res})$ plane. Hence, it is verified that controller (3.1) is indeed robust. This can also be verified by the cost criteria (4.1). Indeed, using the simulation results, it can be observed that for those values of the uncertain parameters that lie within the area where the maximum pendulum angle condition is met, the corresponding values of the cost criteria introduced in (4.1), do not significantly change. Finally in Figure 17, the closed loop pendulum angle response is presented for the cases a) $\delta k_{res} = 0$ and $\delta c_{res} = 0$ and b) $\delta k_{res} / \bar{k}_{res} = 9\%$ and $\delta c_{res} / \bar{c}_{res} = 9\%$. Note that the second case is marginally inside the area where the maximum pendulum angle condition is satisfied. It can be observed that the two responses are visually identical. The same observation holds for all $(\delta k_{res}, \delta c_{res})$ where the maximum pendulum angle condition is satisfied. This is consistent with the fact that the cost criteria (4.1a) and (4.1b) do not significantly change inside that area.

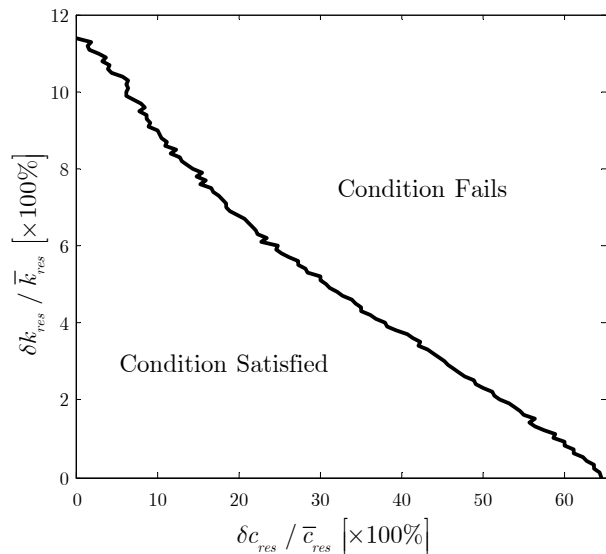


Fig. 16 Robustness analysis for the closed-loop system of the liquid transfer vehicle with uncertain resonator parameters

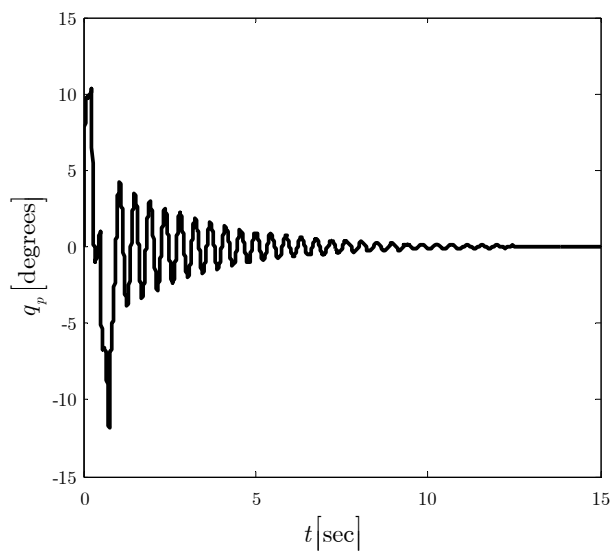


Fig. 17 Closed loop pendulum angle for $\delta k_{res}/\bar{k}_{res} = 0$ and $\delta c_{res}/\bar{c}_{res} = 0$ (continuous) and $\delta k_{res}/\bar{k}_{res} = 9\%$ and $\delta c_{res}/\bar{c}_{res} = 9\%$ (dotted) (visually identical)

4 Conclusions

In the present paper, the dynamic model of the plant presented in [13] has been modified to take into account simultaneous wear to the front and rear springs of the resonator. This failure has been modeled as increase to the spring constant of the resonators with simultaneous decrease to the damping factor. A sloshing suppression control scheme, whose parameters have been evaluated using a metaheuristic approach, designed knowing only the nominal values of the resonator parameters while considering their real values to be unknown, has been applied to the real system. Then, robustness

of the control scheme has been studied under the aforementioned uncertainty in the resonator parameters due to wear. The controller has then been applied to the real system whose parameters may vary from the nominal values.

The contribution of the present paper consists in determining the sets of resonator parameters where the feedback control law produces satisfactory results. It has been observed that there exists a significant area in the $(\delta k_{res}, \delta c_{res})$ plane where the maximum pendulum angle condition is met, while it has been verified that the controller is robust for a wide range of the uncertain parameters.

Acknowledgment

The present work is co-financed by the Hellenic Ministry of Education and Religious Affairs' and the ESF of the European Union within the framework of the "Operational Programme for Education and Initial Vocational Training" (Operation "Archimedes-II").

References

- [1] K. Yano, S. Higashikawa and K. Terashima, "Motion control of liquid container considering an inclined transfer path," *Control Eng. Practice*, vol. 10, pp. 465-472, 2002.
- [2] J. Feddema, C. Dohrmann, G. Parker, R. Robinett, V. Romero and D. Schmitt, Robotically controlled slosh-free motion of an open container of liquid, *1996 IEEE Int. Conf. on Robotics and Automation*, Minneapolis, Minnesota, April 1996, pp. 596-602
- [3] K. Terashima, M. Hamaguchi and K. Yamaura, Modeling and input shaping control of liquid vibration for an automated pouring system, *35th Conf. on Decision and Control*, Kobe, Japan, 1996, pp. 4844-4850
- [4] J. T. Feddema, C. R. Dohrmann, G. G. Parker, R. D. Robinett, V. J. Romero and D. J. Schmitt, Control for slosh-free motion of an open container, *IEEE Control Systems Magazine*, vol. 17, no. 1, pp. 29-36, 1997
- [5] K. Yano and K. Terashima, "Robust liquid container transfer control for complete sloshing suppression," *IEEE Trans. Control Systems Techn.*, vol. 9, pp. 483-493, 2001
- [6] K. Yano, S. Higashikawa and K. Terashima, Liquid container transfer control on 3D transfer path by hybrid shaped approach, *2001 IEEE Int. Conf. on Control Applications*, 5-7, 2001, Mexico City, Mexico, pp. 1168-1173

- [7] K. Yano, T. Toda and K. Terashima, Sloshing suppression control of automatic pouring robot by hybrid shape approach, *40th IEEE Conference on Decision and Control*, Orlando, Florida, USA, December 2001, pp. 1328-1333
- [8] K. Terashima and K. Yano, Sloshing analysis and suppression control of tilting-type automatic pouring machine, *Control Eng. Practice*, vol. 9, pp. 607-620, 2001
- [9] H. Sira-Ramirez, A flatness based generalized PI control approach to liquid sloshing regulation in a moving container, *American Control Conference*, Anchorage, USA, May 8-10, 2002, pp. 2909-2914
- [10] S. Kimura, M. Hamaguchi and T. Taniguchi, Damping control of liquid container by a carrier with dual swing type active vibration reducer, *41st SICE Annual Conference*, 2002, pp. 2385- 2388.
- [11] Y. Noda, K. Yano and K. Terashima, Tracking to moving object and sloshing suppression control using time varying filter gain in liquid container transfer, *2003 SICE Annual Conference*, Fukui, Japan, 2003, pp. 2283-2288
- [12] M. Hamaguchi, K. Terashima, H. Nomura, Optimal control of liquid container transfer for several performance specifications, *J. Advanced Autom. Techn.*, vol. 6, pp. 353-360, 1994
- [13] M.P. Tzamtzi, F.N. Koumboulis, N.D. Kouvakas and G.E. Panagiotakis, A Simulated Annealing Controller for Sloshing Suppression in Liquid Transfer with Delayed Resonators, *14th Mediterranean Conf. on Control and Autom.*, Ancona, Italy, June 2006.
- [14] N. Olgac and B. T. Holm-Hansen, A novel active vibration technique: delayed resonator, *Journal of Sound and Vibration*, vol. 176, no. 1, pp. 93-104, 1994
- [15] N. Olgac, H. Elmali and S. Vijayan, Introduction to the dual frequency delayed resonator, *Journal of Sound and Vibration*, vol. 189, no. 3, pp. 355-367, 1996
- [16] D. Filipovic, N. Olgac, Delayed resonator with speed feedback including dual frequency - theory and experiments, *36th Conf. on Decision and Control*, San Diego, California, USA, Dec. 1997, pp. 2535-2540
- [17] O. Buyukozturk and T.-Y. Yu, Structural Health Monitoring and Seismic Impact Assessment, *5th National Conf on Earthquake Engineering*, Istanbul, Turkey, May 2003
- [18] M.P. Tzamtzi, F.N. Koumboulis, Robustness of a Robot Control Scheme for Liquid Transfer, *Int. Joint Conf. on Comp., Information, and Systems Sciences, and Eng. (CIS²E 07)*, Dec. 2007 // also in *Novel Algorithms and Techniques in Telecommunications, Automation and Industrial Electronics*, T. Sobh et al. (eds), pp. 154-161, Springer, 2008
- [19] M. P. Tzamtzi, F. N. Koumboulis, N.D. Kouvakas, M.G. Skarpetis, "Robustness in Liquid Transfer Vehicles with Delayed Resonators", *6th WSEAS International Conference on Circuit, Systems, Electronics, Control & Signal Processing (CSECS'07)*, pp. 233-238
- [20] F.N. Koumboulis and M.P. Tzamtzi, A metaheuristic approach for controller design of multivariable processes, pp 1429-1432, *12th IEEE International Conference on Emerging Technology on Factory Automation*, Rio-Patras, Greece 2007
- [21] N.D. Kouvakas N.D. Kouvakas, F.N. Koumboulis and P.N. Paraskevopoulos, Modeling and Control of a Test Case Central Heating System, *6th WSEAS International Conference on Circuits, Systems, Electronics, Control & Signal Processing*, Cairo-Egypt, 2007. pp. 289-297
- [22] M. P. Tzamtzi, F. N. Koumboulis, M.G. Skarpetis, "On the Controller Design for the Outpouring Phase of the Pouring Process", *6th WSEAS International Conference on Circuits, Systems, Electronics, Control & Signal Processing (CSECS'07)*, Cairo, Egypt, 2007, pp. 270-277.
- [23] M.R. Jalali, A. Afshar, M.A. Marino, "Ant Colony Optimization Algorithm (ACO); A New Heuristic Approach for Engineering Optimization", *6th WSEAS International Conference on Evolutionary Computing*, Lisbon, Portugal, June 16-18, 2005, pp. 188-192.